Calcium influx through hyperpolarization-activated cation channels (I_h channels) contributes to activity-evoked neuronal secretion

Xiao Yu*†, Kai-Lai Duan*†, Chun-Feng Shang*, Han-Gang Yu‡, and Zhuan Zhou*§

*Institute of Neuroscience, Shanghai Institutes for Biological Sciences, Chinese Academy of Sciences, Shanghai 200031, China; and ‡Department of Physiology and Biophysics, New York College of Osteopathic Medicine, New York Institute of Technology, Old Westbury, NY 11568

Edited by Bert Sakmann, Max Planck Institute for Medical Research, Heidelberg, Germany, and approved December 1, 2003 (received for review August 12, 2003)

The hyperpolarization-activated cation channels (I_h) play a distinct role in rhythmic activities in a variety of tissues, including neurons and cardiac cells. In the present study, we investigated whether Ca^{2+} can permeate through the hyperpolarization-activated pacemaker channels (HCN) expressed in HEK293 cells and I_h channels in dorsal root ganglion (DRG) neurons. Using combined measurements of whole-cell currents and fura-2 Ca^{2+} imaging, we found that there is a Ca^{2+} influx in proportion to I_h induced by hyperpolarization in HEK293 cells. The I_h channel blockers Cs^+ and ZD7288 inhibit both HCN current and Ca^{2+} influx. Measurements of the fractional Ca^{2+} current showed that it constitutes 0.60 ± 0.02% of the net inward current through HCN4 at −120 mV. This fractional current is similar to that of the low Ca^{2+}-permeable AMPA-R (α-amino-3-hydroxy-5-methyl-4-isoxazolepropionic acid receptor) channels in Purkinje neurons. In DRG neurons, activation of I_h for 30 s also resulted in a Ca^{2+} influx and an elevated action potential-induced secretion, as assayed by the increase in membrane capacitance. These results suggest a functional significance for I_h channels in modulating neuronal secretion by permitting Ca^{2+} influx at negative membrane potentials.

As the most important second messenger, Ca^{2+} controls many physiological events, such as neurotransmitter release and muscle contraction (1, 2). Whereas the classic voltage-dependent calcium channels provide an important pathway for Ca^{2+} entry into neurons (3, 4), many ligand-gated cation channels are also permeable to Ca^{2+}, providing another pathway for Ca^{2+} influx (5–8). Fractional Ca^{2+} current, the percentage of current carried by Ca^{2+} in the total current through cation channels, has been determined for nicotinic acetylcholine receptors (nAChRs) (6), for glutamate receptors [*N*-methyl-D-aspartate receptors (NMDA-Rs) and α-amino-3-hydroxy-5-methyl-4-isoxazolepropionic acid receptors (AMPA-Rs)] (7, 9), for cyclic nucleotide-gated (CNG) channels (8), and for voltage-dependent Ca^{2+} channels (VDCC) (3). The Ca^{2+} influx through these channels may result in transmitter release or muscle contraction (e.g., CNG and AMPA-Rs, see refs. 8–10; VDCC and NMDA-Rs, see refs. 3 and 11; and nAChRs and P2X-R, see refs. 12 and 13).

The voltage-dependent hyperpolarization-activated cyclic nucleotide-gated (HCN) channels generate a hyperpolarization-activated cation inward current, named I_h (for hyperpolarization-activated current) in neurons and I_f (for funny current) in cardiac cells. Opened by hyperpolarization, these channels are thought to be permeable only to Na^+ and K^+ ions (14–17). Near the membrane resting potential, I_h channels conduct more Na^+ into and less K^+ out of the cell, generating a net inward current. In rhythmically pacing cells, this inward current contributes to the slow depolarization toward the threshold for firing (4).

Four pore-forming subunits (HCN1 to -4) of I_h channels have been identified in brain (16, 17). They resemble the voltage-gated potassium channel superfamily. HCN channel subunits contain six transmembrane domains (S1–S6), with a pore-forming P region between S5 and S6 (16). All four HCN subunits have an identical pore region, indicating that their ion selectivity should be similar. HCN messenger RNA is widely and nonuniformly expressed in central neurons (18), photoreceptors (19), dorsal root ganglion (DRG) neurons and cardiac myocytes (19, 20).

Recently, I_h channels in neurons have received increasing attention because the activation of I_h affects a variety of neural functions including synaptic plasticity. At the crayfish neuromuscular junction, activation of I_h channels by cAMP or by hyperpolarization induces synaptic facilitation (21). In hippocampal neurons, the presynaptic mossy fiber long-term potentiation (LTP) is also dependent on I_h activation (ref. 22, but see refs. 23 and 24). Biophysical studies have shown that the I_h channel is permeable only to monovalent cations in physiological solutions (25), and I_h-mediated membrane depolarization is not responsible for I_h modulation of synaptic plasticity. Thus, it is not surprising that possible mechanisms for any I_h-mediated events are assumed to be downstream from Ca^{2+} (21, 22). However, this interpretation may need to be revised, considering the possibility of Ca^{2+} influx through the I_h channel itself.

Using a combined whole-cell patch clamp recording and fluorescence Ca^{2+} imaging method, we show that Ca^{2+} permeates through I_h channels. Furthermore, activation of I_h channels causes a marked facilitation of action potential-induced secretion from DRG neurons, as revealed by membrane capacitance measurements. Thus, Ca^{2+} entry through I_h channels may provide a cellular basis for I_h-mediated events, such as presynaptic facilitation and LTP.

NEUROSCIENCE

Materials and Methods

Heterologous Expression of HCN Channels. Human HCN4 subcloned into *Hin*dIII/*Xba*I sites in pcDNA1.1/Amp vector was generously provided by U. B. Kaupp (Forshungszentrum Julich, Germany). HEK293 cells were grown in DMEM, supplemented with 10% FBS, 100 units/ml penicillin, and 100 μg/ml streptomycin. When cells approached confluence, they were seeded into 35-mm dishes and subsequently transfected with the HCN plasmid by using a calcium phosphate method. HCN4 was cotransfected with the GFP to guide selection of cells expressing HCN channels. After 48–96 h, transfected cells with green fluorescence were selected for patch clamp experiments.

Cell Dissociation. Adrenal chromaffin cells from Wistar rats (SLACCAS Inc., Shanghai) were isolated and cultured as de-

This paper was submitted directly (Track II) to the PNAS office.

Abbreviations: NMDA-R, *N*-methyl-D-aspartate receptor; AMPA-R, α-amino-3-hydroxy-5-methyl-4-isoxazolepropionic acid receptor; VDCC, voltage-dependent Ca^{2+} channel; HCN, hyperpolarization-activated cyclic nucleotide-gated; DRG, dorsal root ganglion; Cm, membrane capacitance; LTP, long-term potentiation; HEK, human embryonic kidney; AP, action potential.

†X.Y. and K.-L.D. contributed equally to this work.

§To whom correspondence should be addressed at: Institute of Neuroscience, 320 Yue-Yang Road, Shanghai 200031, China. E-mail: zzhou@ion.ac.cn.

© 2004 by The National Academy of Sciences of the USA

Table 1. Composition of internal solutions* (in mM)

	HEK cells	DRG neurons	Chromaffin cells
NaCl	10	—	—
KCl	145	150†	—
CsCl	—	—	153
$MgCl_2$	1	1	1
Hepes	5	10	5
ATP-Mg	—	4	—
pH	7.2	7.2	7.2

*For fluorescence calibration experiments, 1 mM fura-2 potassium salt was added to internal solutions. For calcium imaging experiments, 0.1 mM fura-2 salt was added to internal solutions.

†For capacitance measurement of DRG neurons, 150 mM KCl was replaced with 153 mM CsCl to block K^+ channels.

scribed (26, 27). Cells were used in the experiments after 2–6 days in culture.

DRG neurons were isolated as described with slight modification and used 4–16 h after preparation (28). We used small- to middle-sized (25–40 μm) neurons.

The use and care of animals used in this study complied with the guidelines of the Animal Research Advisory Committee at the Shanghai Institutes of Biological Sciences.

Electrophysiology. Ionic currents were studied in the whole-cell configuration under voltage-clamp by using an EPC-9 amplifier (HEKA Electronics, Lambrecht/Pfalz, Germany). For switching external solutions, we used an RCP-2B perfusion system, which has a fast exchange time (100 ms) controlled electronically among seven channels (Inbio, Wuhan, China; ref. 28).

Solutions used for experiments are summarized in Tables 1 and 2. Pipette resistances were 2–5 MΩ for human embryonic kidney (HEK) cells, DRG neurons, and adrenal chromaffin cells.

Fluorescence calibration experiments were performed in spherical adrenal chromaffin cells, 12–15 μm in diameter. High CsCl-containing intracellular solution (see Table 1) was used to measure voltage-gated Ca^{2+} currents.

The membrane capacitance measurements were carried out with a software lock-in amplifier of the PULSE software controlling the EPC-9 amplifier (HEKA Electronics; ref. 28). Simulated action potential bursts for stimulation were constructed by computer from an action potential template, which was prerecorded from a DRG neuron under current clamp. This action potential (AP)-stimulation waveform was applied to the DRG neurons under whole-cell voltage-clamp.

DMEM and FBS were purchased from GIBCO. Fura-2 salt was from Molecular Probes. All other chemicals were from Sigma. All experiments were conducted at room temperature (22–24°C).

Fluorescence Measurements and Theory of Fractional Ca^{2+} Measurements. Intracellular calcium ($[Ca^{2+}]_i$) was measured by using a Ca^{2+} imaging system (TILL Photonics, Planegg, Germany).

Table 2. Composition of external solutions (in mM)

	HEK cells	DRG neurons	Chromaffin cells
NaCl	138	150	—
NMG	—	—	138
KCl	5.6	5	5.6
$CaCl_2$	2.6	2.5	2.6
$MgCl_2$	1.2	1	1.2
Hepes	10	10	10
Glucose	10	10	10
pH	7.4	7.4	7.4

Fura-2 (0.1–1.0 mM) was loaded into the cell via a patch-pipette in the whole-cell configuration. The fluorescence was sampled at a frequency of 1 Hz (28).

Fractional Ca^{2+} current, *Pf*, is defined as the percentage of Ca^{2+} current in the total current passing through a cation channel (say, I_{HCN4} in this case). According to the original definition (6),

$$Pf = \int I_{HCN,Ca}\,dt \Big/ \int I_{HCN}\,dt = \Delta Fd/(f_{max}\cdot\int I_{HCN}\,dt)\,, \quad [1]$$

where I_{HCN} is the HCN4 current, and $I_{HCN,Ca}$ is the proposed fractional I_{HCN4} current carried by Ca^{2+}. ΔFd is the change of *Fd*, which is the "modified Ca^{2+}-sensitive fura-2 signal" immediately before (Fd') and after (Fd'') the voltage-pulse induced Ca^{2+} influx (3), Fd = F340 −F380, $\Delta Fd = Fd'' - Fd'$, and f_{max} is a constant, which is determined by measuring Ca^{2+} influx through voltage-gated calcium channels in chromaffin cells under the condition that intracellular fura-2 is sufficiently high (>0.4 mM) (6). Under physiological conditions, all ions contributing to the current through Ca^{2+} channels are Ca^{2+} (3), or $Pf = 100\%$. From Eq.**1**, we have $f_{max} = \Delta Fd/(\int I_{Ca}\,dt)$, where I_{Ca} is the current through voltage-gated Ca^{2+} channels.

To record the time course of fura-2 dialysis, following ref. 6, we used the Ca^{2+}-independent fluorescence signal F360, which can be calculated from F340 and F380. F360 = F340 + αF380, where α is the "isocoefficient" and can be determined by any experimental recording that shows rapid changes in Ca^{2+} concentration. In our setup, α = 0.35. Because F360 is Ca^{2+} independent, it can be used as an indicator of the intracellular fura-2 concentration $[fura]_i$. After establishing the whole-cell recording configuration, fura-2 was dialyzed into the cell, and this was accompanied by a proportional F360 increase. Once F360 reached a steady-state level, we assumed that $[fura]_i$ was equal to the fura-2 concentration in the pipette (see Fig. 3 and ref. 6).

According to Eq. **1**, by measuring the fura-2 signal evoked after activation of I_{HCN4} in HEK293 cells expressing HCN channels, the *Pf* of HCN channels can be determined.

Intracellular free Ca^{2+} concentration, $[Ca^{2+}]_i$, was measured according to Grynkiewicz *et al*. (29): $[Ca^{2+}]_i = K_{eff}\cdot(R - R_0)/(R_1 - R)$, where R_0 = 0.1, R_1 = 3.4, and K_{eff} = 1938 nM, as determined by standard calibrations (29, 30).

Data were analyzed with IGOR PRO-3.12 software (WaveMetrics, Lake Oswego, OR). Unless otherwise stated, the data were presented as mean ± SD. Statistical significance was tested with Student's *t* test. $P < 0.05$ was considered statistically significant.

Results

To explore Ca^{2+} permeation through I_h channels, we first needed a simple expression system with the least contamination by other ion channels. We chose human embryonic kidney (HEK293) cells in which the expression of endogenous voltage-gated ion channels, including I_h channels, is either undetectable or very small compared with that in excitable cells.

Fig. 1 provides a typical example of the hyperpolarization-activated current in a HEK cell expressing HCN 4. Fig. 1*A* shows the currents induced by HCN4 channels (I_{HCN4}) in response to 10-s hyperpolarizing pulses from −50 to −120 mV in 10-mV increments (holding potential, −40 mV). To determine the reversal potential, a prehyperpolarizing pulse to −120 mV was applied to fully activate I_{HCN4}, and the membrane was then clamped back to test pulses ranging from −70 to −20 mV for 1.5 s. The reversal potential was determined by plotting the amplitudes of tail currents (Fig. 1*B Upper*) against the test potentials. Averaging over six cells, the reversal potential of HCN4 was −37 mV (Fig. 1*B Lower*). At −120 mV, the time

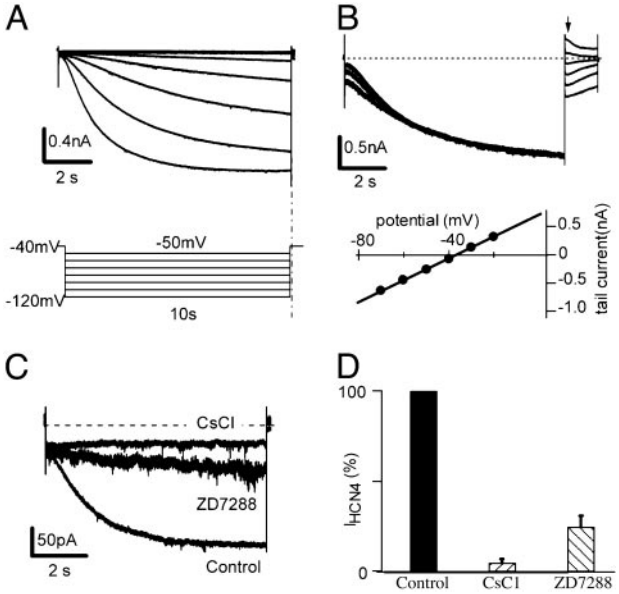

Fig. 1. Properties of HCN channels expressed in HEK293 cells. (*A*) HCN4 currents (I_{HCN4}, *Upper*) and voltage protocol (*Lower*). Cells expressing HCN4 were clamped from −40 mV to various voltages (−120 to −50 mV in 10-mV increments) for 10 s. (*B*) Determination of reversal potential of HCN4. An 8-s prepulse to −120 mV was applied to fully activate I_{HCN4}. Test pulses of 1.5 s ranging from −70 to −20 mV in 10-mV increments were then applied to deactivate I_{HCN4}. (*Upper*) A typical series of I_{HCN4} where the dashed line indicates zero current. The arrow indicates the start of the test pulses. By plotting the tail currents against the test potentials, the reversal potential of −37 mV was determined (*Lower*, $n = 6$). (*C*) Inhibition of I_{HCN4} by extracellular application of Cs^+ (2 mM) or ZD7288 (30 μM). I_{HCN4} were evoked from −40 mV to −120 mV for 10 s and inhibited by Cs^+ or by ZD7288. (*D*) Statistics of I_{HCN4} blockade by CsCl (2 mM) or ZD7288 (30 μM). Cesium blocked 95 ± 3% ($n = 4$) and ZD7288 blocked 75 ± 6% ($n = 6$) of I_{HCN4}.

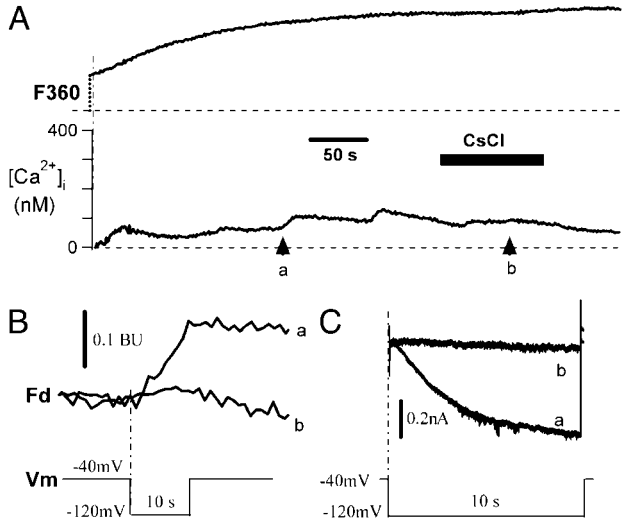

Fig. 2. Cs^+ blockade of Ca^{2+} influx through HCN4 channels in HEK293 cells. (*A*) Ca^{2+} signals in response to hyperpolarizing pulses in the absence and presence of 2 mM CsCl. Two of the pulse-induced Ca^{2+} signals are analyzed below. Similar results were observed in all three cells tested. The dashed lines are baselines. (*B*) *Fd* signals corresponding to arrows a and b in *A*. (*C*) I_{HCN4} (trace a) was blocked by 2 mM Cs^+ (trace b). Dashed line represents zero current. (*Lower*) The voltage protocol is shown.

constant of activation was 2.4 ± 0.3 s ($n = 12$). I_{HCN4} was blocked by Cs^+ and a selective I_h channel blocker, ZD7288 (21) (Fig. 1*C*). The currents were elicited by a hyperpolarizing pulse to −120 mV for 10 s from a holding potential of −40 mV. Application of 2 mM CsCl to the external solution blocked I_{HCN4} whereas 30 μM ZD7288 inhibited the current. On average, 2 mM Cs^+ blocked 95 ± 3% ($n = 4$) of the I_{HCN4} whereas ZD7288 (30 μM) blocked 75 ± 3% (Fig. 1*D*, $n = 6$). The currents generated by HCN channel activation are largely insensitive to Ba^{2+} (which is widely used for blocking a variety of K^+ currents; data not shown). The results are consistent with the typical properties of HCN4 expressed in HEK cells (31).

Fig. 2 presents an example of the fluorescence signals (F360 and $[Ca^{2+}]_i$, Fig. 2 *A* and *B*) and the HCN4 currents expressed in a HEK293 cell in response to a step to −120 mV from a holding potential of −40 mV (Fig. 2*C*). Surprisingly, there was $[Ca^{2+}]_i$ rise during activation of HCN4 channels, implying existence of Ca^{2+} influx through the cation channel. When the HCN4 current (Fig. 2*C*, trace a) was blocked by Cs^+ (Fig. 2*C*, trace b), the simultaneous increase in $[Ca^{2+}]_i$ (Fig. 2*A*, arrow a) was also eliminated in the presence of Cs^+ (Fig. 2*A*, arrow b). *Fd* changes in the absence and presence of Cs^+ are illustrated in Fig. 2*B*.

Fig. 3 shows the protocol used to determine Ca^{2+} permeation through HCN4 channels expressed in HEK293 cells. A high concentration of fura-2 (1 mM), the calcium-sensitive fluorescent probe, was included in the patch-pipette and loaded into the cell in a whole-cell patch configuration. Entry of fura-2 into the cell was monitored by the Ca^{2+}-insensitive signal, F360 (Fig. 3*A*, top traces). On binding to Ca^{2+}, the fluorescence signal at F380 (Fig. 3*A*, middle traces) and the modified Ca^{2+}-sensitive *Fd* (Fig. 3*B*, top traces, see *Materials and Methods*) were used to detect the net Ca^{2+} influx through voltage-gated calcium channels (Fig. 3*A*, right bottom trace) and HCN4 channels (Fig. 3*A*, left bottom trace). When intracellular fura-2 concentration $[Ca^{2+}]_i$ is higher than 0.4 mM, the buffering capacity of fura-2 out-competes the endogenous Ca^{2+} buffers so that all inflowing Ca^{2+} is bound by fura-2 and reported by the Ca^{2+}-sensitive *Fd* signals (3, 6).

Fig. 3 *B* and *C* illustrates how the fractional Ca^{2+} current (*Pf*) of the HCN4 channel was obtained by using Eq. **1** (see *Materials and Methods*). In Fig. 3*B Right*, we show that, in a rat adrenal chromaffin cell (RACC), a depolarizing step to 0 mV from a holding potential of −70 mV activated a voltage-dependent Ca^{2+} current (VDCC) and simultaneously induced an increase in Fd (ΔFd2, Fig. 3*B*, top trace). The shaded region marks the area over which the time integral of the ion flux through the calcium channels was calculated. In *Left*, we show that, in a HEK293 cell, a hyperpolarizing step to −120 mV from a holding potential of −40 mV activated the HCN4 current (middle trace), and simultaneously induced an increase in *Fd* (Δ*Fd1*, top trace). The shaded region defines the time integral of ion flux through HCN4 channels. Fig. 3*C* shows the relationship between total ion influx and the corresponding increase in *Fd* (Δ*Fd*) obtained with different durations of stimulation. Data were best fitted by a linear equation, indicating a correlation between the increased Δ*Fd* and the increased ion flux for both VDCC and HCN4. The ratio, defined as Δ*Fd* over ion influx (Fig. 3*C Inset*), is ≈200 times larger for voltage-gated Ca^{2+} channels (*k1*) than for HCN4 channels (*k2*). Using Eq. **1**, we determined *Pf* to be 0.60 ± 0.02% of total I_{HCN4} ($n = 9$, Fig. 3*D*).

We have thus far shown that (*i*) activation of HCN4 can simultaneously induce an increase in *Fd* that indicates net Ca^{2+} influx and (*ii*) when HCN4 is blocked by Cs^+, the concomitant increase in Fd is also blocked. These results strongly suggest that the hyperpolarization-induced Ca^{2+} influx is likely caused by a fractional Ca^{2+} current through open HCN channels.

To extend our observations on calcium permeation through I_h channels to normal cells, we performed similar experiments in DRG neurons where I_h channels (32) and HCN messenger RNA have been detected (19). In whole-cell recording of small- to medium-sized (25–40 μM) C-type DRG neurons, we recorded

NEUROSCIENCE

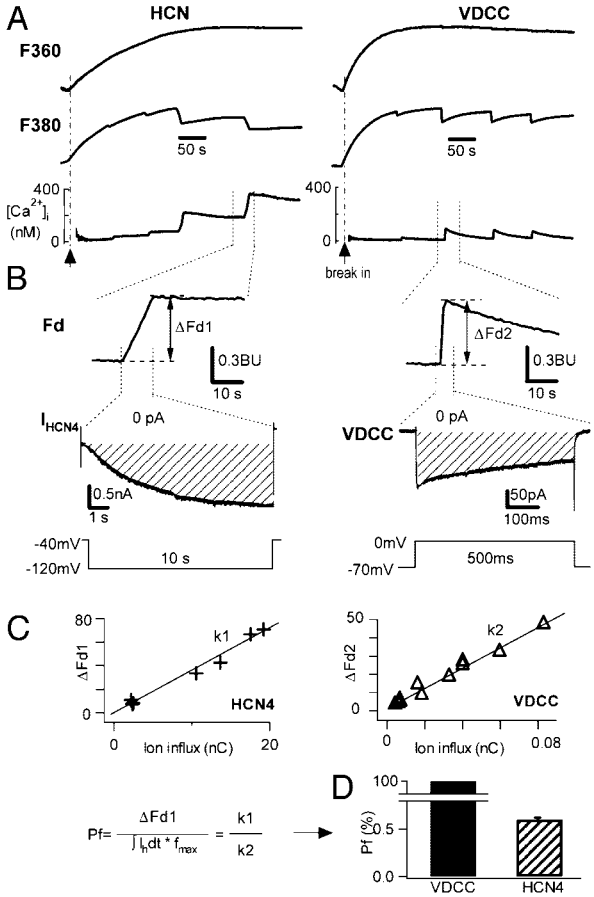

Fig. 3. Protocols to measure Ca^{2+} influx through HCN4 channels. (*A*) Ca^{2+} signals in response to depolarizing pulses (*B Bottom Right*) in a chromaffin cell (voltage-gated Ca^{2+} current, VDCC, *Right*) and to hyperpolarizing pulses (*B Bottom Left*) in a HEK293 cell expressing HCN4 (HCN, *Left*). Ca^{2+} signals during fura-2 loading (1 mM in the pipette) F360 (top traces, indicating fura-2 entry into the cell), F380 (middle traces, indicating Ca^{2+} influx), and $[Ca^{2+}]_i$ (bottom traces) are shown. Dashed lines are baselines. (*B*) Ca^{2+} current (*Right*) and I_{HCN4} (*Left*) with the corresponding *Fd* (top traces). *Fd* changes induced by the voltage protocols (*Bottom*) are shown as $\Delta Fd1$ and $\Delta Fd2$ for HCN4 and VDCC, respectively. Dashed lines in current traces indicate zero. The shaded areas indicate the total ion influx charge through the channels. (*C*) Determination of the fractional Ca^{2+} current through HCN4 channels. $\Delta Fd1$ for HCN4 and $\Delta Fd2$ for VDCC are plotted against the ion influx. (*Inset*) The equation used to calculate *Pf* (see *Materials and Methods*). (*D*) Compared with VDCC (*Pf* = 100%) in chromaffin cells (3), the *Pf* of HCN4 is 0.60 ± 0.02% ($n = 7$).

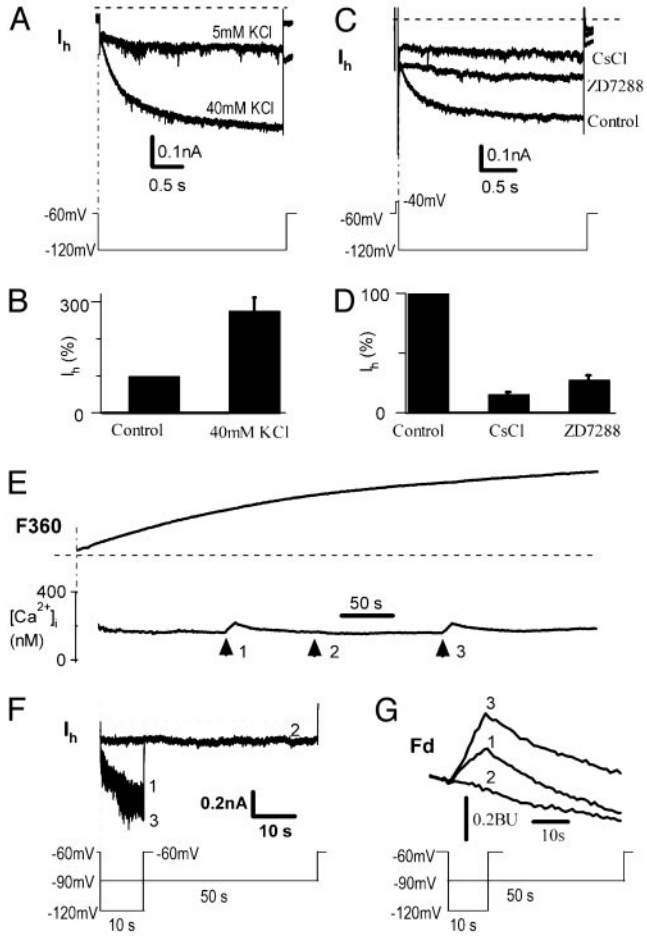

Fig. 4. Ca^{2+} influx through I_h channels in DRG neurons. (*A*) Enhancement of I_h by increasing $[K^+]_o$ from 5 to 40 mM in a neuron. The pulse protocol is shown below. (*B*) Normalized I_h is increased by 277 ± 34% in 40 mM vs. 5 mM KCl ($P < 0.001$, $n = 6$). (*C*) Inhibition of hyperpolarization-induced I_h by extracellular Cs^+ (2 mM) or ZD7288 (30 μM). (*D*) I_h was blocked significantly by 2 mM CsCl (84 ± 3%; $P < 0.01$, $n = 11$) or 30 μM ZD7288 (75 ± 5%, $P < 0.01$, $n = 5$). (*E*) Ca^{2+} signals in response to hyperpolarizing pulses of −120 mV for 10 s (arrows 1 and 3) or −90 mV for 50 s (arrow 2) in a DRG neuron ($n = 15$). (*F*) I_h at −120 mV for 10 s (traces 1 and 3) and at −90 mV for 50 s (trace 2). Protocols are shown in the text. (*G*) *Fd* signals corresponding to arrows 1, 2, and 3 in *E* and *F*. Similar to HCN4 in HEK293 cells, the fractional Ca^{2+} current of I_h was 0.5 ± 0.1% in DRG neurons ($n = 3$).

typical I_h currents (Fig. 4). The I_h was enhanced by elevating external potassium concentration, $[K^+]_o$, from 5 mM to 40 mM (Fig. 4*A*), a well-known feature of I_h (15). Averaging over six neurons, I_h increased 277 ± 34% ($n = 6$, $P < 0.01$) in response to an 8-fold increase in $[K^+]_o$ (Fig. 4*B*). The hyperpolarizing currents were blocked by Cs^+ (2 mM) and ZD7288 (30 μM) (Fig. 4*C*). The average inhibition was 84 ± 3% ($n = 11$, $P < 0.01$) by Cs^+ and 75 ± 5% ($n = 5$, $P < 0.01$) by ZD7288 (Fig. 4*D*). The activation time constant of I_h in DRG neurons was 0.51 ± 0.05 s ($n = 15$), which is faster than HCN4 channels (2.35 s, Fig. 1). The activation time constant of 0.51 s is consistent with HCN1 and HCN2, which are the major components of I_h in rat DRG neurons and have time constants of 0.03–0.2 s (19).

Similar to reconstituted HCN channels, activation of I_h channels by hyperpolarization to −120 mV induces Ca^{2+} influx into DRG cells. Fig. 4*E* shows an example of I_h activation and the associated fluorescence changes recorded in a DRG neuron. In response to a hyperpolarizing step to −120 mV for 10 s from a holding potential of −60 mV, I_h was activated (Fig. 4*F*, traces 1 and 3), and accompanied by increases in $[Ca^{2+}]_i$ (Fig. 4*E*, arrows 1 and 3, and Fig. 4*G*). When a weaker hyperpolarizing pulse to −90 mV was applied for 50 s, I_h was not activated (Fig. 4*F*, trace 2, and Fig. 4*G*), and no change in $[Ca^{2+}]_i$ was observed (Fig. 4*E*, arrow 2).

To investigate the physiological relevance of the Ca^{2+} influx through I_h channels, we used Cm (membrane capacitance) to measure AP-induced secretion before and after activation of I_h channels in DRG neurons (28). We recorded a typical AP and used it as a template to build a burst of 10 APs at 100 Hz (Fig. 5*A Inset*) and applied the AP burst to the voltage-clamped cell. The computer-constructed AP burst induced a capacitance increase of 0.57 pF (Fig. 5*A*), which corresponds to the exocytosis of 1,140 vesicles (vesicle diameter 140 nm, corresponding to 0.5 fF/vesicle; ref.28). The stimulation-induced changes in Gs (whole-cell series conductance) and Gm (membrane conductance) were negligible, indicating that the lock-in assay of Cm is accurate (33). The neuron was stimulated four times with eight

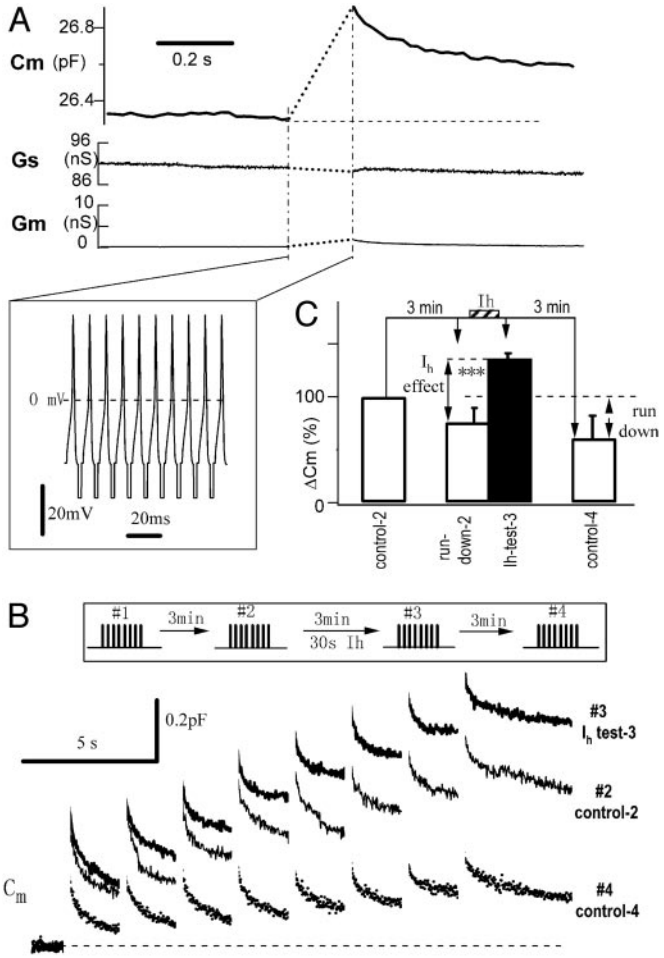

Fig. 5. I_h modulation of AP-induced exocytosis in DRG neurons. (*A*) An AP burst (*Inset*) induced a Cm rise in a DRG neuron. (*B*) I_h facilitates AP-induced secretion. Cm traces were recorded as #1 (control-1, data not shown), #2 (control-2, after 3 min rundown), #3 (test-3, after activation of I_h), and #4 (control-4, without I_h activation) at 3-min intervals. Cm traces #2, #3, and #4 are overlapped for comparison. (*C*) Statistical analysis over 10 experiments. Note that the total Cm change induced by an AP train depends not only on exocytosis, but also on endocytosis after each Cm jump. To reduce this effect, secretion induced by an AP train was indicated by ΔCm, which was the sum of Cm jumps immediately after each AP burst. Three minutes after the third stimulation, the AP-induced secretion was decreased to 61 ± 21% of the control-2 level ($P < 0.01$, $n = 10$).

AP bursts separated by 2-s intervals (i.e., 80 APs each time; Fig. 5*B Inset*). Three minutes after the first set of stimuli (control-1, data not shown), the second stimulation (Fig. 5*B*, control-2) showed a 16% rundown. To test the effect of I_h on AP-induced Cm, immediately before applying the third AP series, the neuron was hyperpolarized to −120 mV for 30 s. The third stimulation evoked a Cm response (Fig. 5*B*, I_h test-3), which was 43% larger than control-2. Finally, 3 min later, the fourth stimulation evoked a response (Fig. 5*B*, control-4), which was 59% smaller than control-2. Similar results were observed in all cells tested. On average, activation of I_h for 30 s increased AP-induced secretion to 136 ± 5% of control ($P < 0.001$, $n = 10$). This is an underestimate because of the 24 ± 14% rundown (comparing control-1 and -2) during the 3-min whole-cell recording. If the rundown effect is compensated, the total facilitation of AP-induced secretion would be 179 ± 19% ($P < 0.001, n = 10$, paired *t* test). Thus, consistent with the findings from the crayfish neuromuscular junction (21), activation of I_h channels enhances AP-induced secretion from DRG neurons. Activation of *I*h was responsible for the facilitation because 2 mM Cs^+ blocked both I_h currents and AP-induced Cm facilitation ($n = 5$, data not shown). Ca^{2+} influx through I_h channels is most likely the mechanism underlying the facilitation of AP-induced secretion in DRG neurons because combined measurements of fura-2 fluorescence Ca^{2+} imaging and patch-clamp Cm recording revealed that activation of I_h increased the basal Ca^{2+}, and the subsequent AP-induced $[Ca^{2+}]_i$ and Cm (Fig. 6, which is published as supporting information on the PNAS web site, and data not shown). These experiments strongly suggest that Ca^{2+} inflow through I_h channels is responsible for the I_h-induced facilitation in DRG neurons.

Discussion

We have shown that HCN channels are permeable to Ca^{2+}. Brief activation of I_h in DRG neurons nearly doubles the action potential-induced secretion from DRG neurons. Thus, the fractional Ca^{2+} influx through the slow I_h channels may affect Ca^{2+}-dependent synaptic transmission.

Permeability of HCN Channels to Ca^{2+}. I_h channels are widely expressed in peripheral and central neurons as well as in cardiac myocytes. The distinct properties of I_h are believed to be associated with a variety of physiological events (25, 34). The discovery of calcium permeation through I_h channels could provide a novel mechanism coupling membrane hyperpolarization with I_h-mediated events.

The fractional Ca^{2+} current of the HCN4 channel (0.6%) is small compared with other Ca^{2+}-permeable channels such as the nicotinic acetylcholine receptor (2.5%) (6), the NMDA-R (8–10%) (7, 9), the non-NMDA-R (0.5–5%) (7, 9), cyclic nucleotide-gated channels (>10%) (35), and L-type Ca^{2+} channels (100%) (3). However, I_h channels have slow kinetics and are activated during the long interval between two action potentials or bursts of action potentials. Under certain experimental conditions, the accumulated fractional Ca^{2+} current through I_h channels could be sufficient to modulate Ca^{2+}-dependent cellular functions, such as neurotransmitter release from DRG neurons (Fig. 6).

I_h channels are permeable to both Na^+ and K^+ ions. Evidence from myocytes has shown that ion permeation although I_h channels does not fully obey the Goldman–Hodgkin–Katz (GHK) equation (15). The independent ion permeation through a multiple-cation channel, an assumption for using the GHK equation, apparently does not work for I_h channels. Our discovery of Ca^{2+} permeation through I_h channels provides an additional piece of evidence for the idea that precautions must be taken when applying the GHK equation to channels that are permeable to multiple ions.

Role of Ca^{2+} Influx Through I_h Channels in Neurons. Two general mechanisms have been proposed for synaptic facilitation: enhanced presynaptic calcium rise (Ca^{2+}-dependent) and direct modulation of the release process (Ca^{2+}-independent). In chromaffin cells and at many synapses, accumulation of presynaptic Ca^{2+} by higher frequencies of action potentials can facilitate synaptic transmission (26, 36–38).

In hippocampal mossy fibers, activation of cAMP/PKA mediates a form of presynaptic LTP, which is interpreted as a Ca-independent process, although the molecular mechanism remains unresolved. One report postulates that I_h is responsible for cAMP-dependent LTP because the I_h antagonist ZD7288 blocks the LTP (22) whereas two other reports argue that the block could be due to side-effects of ZD7288 so I_h is not involved in LTP (23, 24).

Other evidence for a Ca^{2+}-independent mechanism has come from studies of 5-HT action at the crayfish neuromuscular

junction (21). These studies showed that enhanced release induced by 5-HT is not due to PKA activation; the 5-HT-induced depolarization is dramatically inhibited by both Cs^+ and ZD7288, in agreement with the pharmacological profile of I_h; and the activation of I_h by hyperpolarization is sufficient to enhance synaptic transmission. Thus, these workers suggested that the downstream event is probably due to direct interaction between I_h channels and vesicles, i.e., by means of a Ca^{2+}-independent mechanism. In contrast to the study on mossy fiber LTP, which depended on the use of ZD7288, the hyperpolarization-mediated facilitation in crayfish was shown to be mediated by I_h channels (figure 8 of ref. 21) in experiments that did not require the use of this compound. Thus, the hyperpolarization-induced facilitation in crayfish observed by Beaumont and Zucker (21) was probably due to Ca influx through I_h channels.

Our results show that Ca^{2+} ions can pass through I_h channels and significantly elevate cytosolic Ca^{2+} levels. In DRG neurons, the amplitude of I_h is ≈20% of the 1 nA voltage-gated Ca^{2+} current (Fig. 4) so the Ca^{2+} inflow during a 60-s activation of I_h would be equivalent to the Ca^{2+} influx induced by a 72-ms (20%·0.6%·60 s) depolarization through voltage-gated Ca^{2+} channels (or 24 action potentials of 3 ms duration). The I_h-mediated Ca^{2+} increase may facilitate subsequent stimulus-induced secretion in two ways. First, like the facilitation induced by a high action-potential frequency (26, 36), the elevated basal Ca^{2+} assists the cell in secretion. Second, in contrast to voltage-gated Ca^{2+} channels or Ca^{2+} stores that both trigger secretion on stimulation (38), I_h channels could be a more effective pathway for increasing the readily releasable vesicle pool (RRP), because the slow influx of Ca^{2+} through the I_h channel is probably not sufficient to trigger secretion but ensures the increase of the RRP (39). Thus, Ca^{2+} influx through I_h channels provides a mechanism for I_h-mediated synaptic plasticity. Interestingly, the fractional Ca^{2+} current of I_h is close to that of the low Ca^{2+}-permeable AMPA-R channels in Purkinje neurons (40). This result implies that low Ca^{2+} permeation cation channels may play important roles in synaptic transmission.

We note that, although we favor the hypothesis that Ca^{2+} influx through I_h channels is responsible for the facilitation of AP-induced secretion found in this work (as well as the synaptic facilitation induced by hyperpolarization at the crayfish neuromuscular junction; ref.21), we cannot exclude other possibilities, such as a direct link between I_h channels and some factor(s) downstream from Ca^{2+} (21–24). In addition, although the 30-s hyperpolarization is sufficient to induce AP-induced facilitation of cell secretion, it is not clear whether such hyperpolarization occurs in DRG neurons *in vivo*. However, in pacemaker neurons (such as thalamic neurons) or cardiac cells, where I_h is cyclically activated, Ca^{2+} influx through I_h channels may modulate Ca^{2+}-dependent synaptic transmission or heartbeat.

Mechanism of Ca^{2+} Permeation Through I_h Channels. Ca^{2+} must pass through the pore region of I_h channels because blockade of I_h also eliminates the Ca^{2+} influx. The four HCN channels (HCN1 to -4) share the same pore region (16), implying that the Ca^{2+} permeation of HCN1 to -4 channels (including I_h in DRG neurons, Figs. 4 and 5) are probably similar (i.e., Pf = 0.6%). However, we do not yet know the mechanism by which calcium permeates I_h channels. The molecular mechanism of Ca^{2+} permeation through I_h channels might be distinct from that of glutamate channels. In NMDA and AMPA channels, the fractional Ca^{2+} current increases 5-fold when external [Ca^{2+}] is increased from 2 to 10 mM (9). The critical Q/R site for Ca^{2+} permeation through glutamate channels is thus not saturated in bathing solutions containing 2–10 mM Ca^{2+}. In contrast, the Pf of HCN channels is unchanged when external [Ca^{2+}] is changed from 2 to 20 mM (X.Y. and Z.Z., unpublished observations). This finding implies that Ca^{2+} may have saturated at some unknown Ca^{2+} binding site(s) in the I_h channel pore. Future work is needed to determine the critical site(s) in I_h channel proteins that are responsible for Ca^{2+} permeation.

We thank Drs. I. Bruce, M. M. Poo, and H. P. Cheng for suggestions on the manuscript. This work was supported by grants from the Major State Basic Research Program of China (Grant G2000077800), the National Natural Science Foundation of China (Grant 30330210), the Chinese Academy of Sciences Instrument Program, and the Science and Technology Commission of Shanghai Municipality.

1. Katz, B. (1969) *The Release of Neural Transmitter Substances* (Thomas, Springfield, IL).
2. Bers, D. M. (2002) *Nature* **415,** 198–205.
3. Zhou, Z. & Bers, D. M. (2000) *J. Physiol. (London)* **523,** 57–66.
4. Hille, B. (2001) *Ionic Channels in Excitable Membranes* (Sinauer, Sunderland, MA), 3rd Ed.
5. Mayer, M. L. & Westbrook, G. L. (1987) *J. Physiol. (London)* **394,** 501–527.
6. Zhou, Z. & Neher, E. (1993a) *Pflügers Arch*. **425,** 511–517.
7. Schneggenburger, R., Zhou, Z., Konnerth, A. & Neher, E. (1993) *Neuron* **11,** 133–143.
8. Dzeja, C., Hagen, V., Kaupp, U. B. & Frings, S. (1999) *EMBO J*. **18,** 131–44.
9. Burnashev, N., Zhou, Z., Neher, E. & Sakmann, B. (1995) *J. Physiol. (London)* **485,** 403–418.
10. Finn, J. T., Grunwald, M. E. & Yau, K, W. (1996) *Annu. Rev. Physiol*. **58,** 395–426.
11. Koh, D. S., Geiger, J. R., Jonas, P. & Sakmann, B. (1995) *J. Physiol. (London)* **485,** 383–402.
12. Mollard, P., Seward, E. P. & Nowycky, M. C. (1995) *Proc. Natl. Acad. Sci. USA* **92,** 3065–3069.
13. Rogers, M. & Dani, J. A. (1995) *Biophys. J*. **68,** 501–506.
14. DiFrancesco, D. (1993) *Annu. Rev. Physiol*. **55,** 455–472.
15. Yu, H. G., Chang, F. & Cohen, I. S. (1995) *J. Physiol. (London)* **485,** 469–483.
16. Santoro, B., Liu, D. T., Yao, H., Bartsch, D., Kandel, E. R., Siegelbaum, S. A. & Tibbs, G. R. (1998) *Cell* **93,** 717–729.
17. Ludwig, A., Zong, X., Jeglitsch, M., Hofmann, F. & Biel, M. (1998) *Nature* **393,** 587–591.
18. Santoro, B., Chen, S., Luthi, A., Pavlidis, P., Shumyatsky, G. P., Tibbs, G. R. & Siegelbaum, S. A. (2000) *J. Neurosci*. **20,** 5264–5275.
19. Moosmang, S., Stieber, J., Zong, X., Biel, M., Hofmann, F. & Ludwig, A. (2001) *Eur. J. Biochem*. **268,** 1646–1652.
20. Shi, W., Wymore, R., Yu, H. G., Wu, J. Y., Wymore, R., Pan, Z., Robinson, R. B., Dixon, J. E., McKinnon, D. & Cohen, I. S. (1999) *Circulation Res*. **85,** e1–e6.
21. Beaumont, V. & Zucker, R. S. (2000) *Nat. Neurosci*. **3,** 133–141.
22. Mellor, J., Nicoll, R. A. & Schmitz, D. (2002) *Science* **295,** 143–147.
23. Chevaleyre, V. & Castillo, P. E. (2002) *Proc. Natl. Acad. Sci. USA* **99,** 9538–9543.
24. Kamiya, H., Umeda, K., Ozawa, S. & Manabe, T. (2002) *J. Neurosci*. **22,** 10524–10528.
25. Siegelbaum, S. (2000) *Nat. Neurosci*. **3,** 101–102.
26. Zhou, Z. & Misler, S. (1995) *J. Biol. Chem*. **270,** 3498–3505.
27. Wu, J. J., He, L. L., Zhou, Z. & Chi, Z. W. (2002) *Biochemistry* **41,** 2844–2849.
28. Zhang, C. & Zhou, Z. (2002) *Nat. Neurosci*. **5,** 425–430.
29. Grynkiewicz, G., Poenie, M. & Tsien, R. Y. (1985) *J. Biol. Chem*. **260,** 3440–3450.
30. Zhou, Z. & Neher, E. (1993b) *J. Physiol. (London)* **469,** 245–273.
31. Ludwig, A., Zong, X., Stieber, J., Hullin, R., Hofmann, F. & Biel, M. (1999) *EMBO J*. **18,** 2323–2329.
32. Birch, B. D., Kocsis, J. D., Di Gregorio, F., Bhisitkul, R. B. & Waxman, S. G. (1991) *J. Neurophysiol*. **66,** 719–728.
33. Gillis, K. D. (1995) in *Single Channel Recording*, eds. Sakmann, B. & Neher E. (Plenum, New York), 2nd Ed., pp. 155–198.
34. Gauss, R., Seifert, R. & Kaupp UB. (1998) *Nature* **393,** 583–587.
35. Frings, S., Seifert, R., Godde, M. & Kaupp UB. (1995) *Neuron* **15,** 169–179.
36. Zucker, R. S. (1973) *J. Physiol. (London)* **229,** 787–810.
37. Elhamdani, A., Zhou, Z. & Artalejo, C. R. (1998) *J. Neurosci*. **18,** 6230–6240.
38. Augustine, G. J. & Neher, E. (1992) *J. Physiol. (London)* **450,** 247–271.
39. von Ruden, L. & Neher, E. (1993) *Science* **262,** 1061–1065.
40. Tempia, F., Kano, M., Schneggenburger, R., Schirra, C., Garaschuk, O., Plant, T. & Konnerth A. (1996) *J. Neurosci*. **16,** 456–466.